

## PREPARATION OF ACTIVATED CARBON FROM MUSTARD SEED AND ITS ADSORPTION EFFICIENCY TOWARDS DYE AND ACID

Deepa Basrur and J. Ishwara Bhat\*

*Department of Chemistry, Mangalore University, Mangalagangothri – 574199, Karnataka, India*

Received 10 May 2018; received in revised form 16 October 2018; accepted 18 November 2018

### Abstract:

In this work, activated carbon obtained from agro- based material, mustard seeds were used as an adsorbent for the adsorption study of crystal violet (CV) and citric acid (CA). The characterization of synthesized carbon material was performed by various techniques, such as FTIR, SEM, TGA and XRD. FTIR absorption bands of activated carbon exhibited the presence of functional groups on the surface of activated carbon and SEM images showed the impregnation of the pores on the surface of the synthesized activated carbon. Adsorption experiments were conducted to study its capacity as an adsorbent, under various conditions such as concentration, agitation time and temperature. The data acquired from concentration variation found to fit well with Freundlich isotherm. It was shown that the adsorption of dye and acid were better described by the second order kinetic model. Positive values of  $\Delta H_o$  indicated that the process is endothermic and negative values of  $\Delta G_o$  confirmed feasibility of the system. The results showed that microwave activated carbon was more effective for the removal of crystal violet.

### Keywords:

Activated carbon; adsorption; citric acid; crystal violet; Freundlich; interaction; kinetic; Langmuir; microwave; thermodynamic

© 2018 Journal of Urban and Environmental Engineering (JUEE). All rights reserved.

\* Correspondence to: J. Ishwara Bhat, E-mail: [bhatij08@gmail.com](mailto:bhatij08@gmail.com)

## INTRODUCTION

The term adsorption refers to the existence of a higher concentration of any particular component at the surface of a liquid or solid phase than is present in the bulk (Glasstone, 1981). The extent of adsorption depends upon the pore size, pore volume and the exposed surface area of the adsorbent. As activated carbon has a larger surface area in relation to mass (Sawyer *et al.*, 1994), it acts as an effective and resourceful adsorbent and utilized in various sectors for gas purification, water purification, decolourization, metal extraction, medicine, sewage treatment etc. (Raj, 1991). Physical and chemical activation are the two basic methods for the preparation of activated carbons (Song *et al.*, 2012).

Physical activation involves heating the sample at high temperature in presence of steam or carbon dioxide where as in chemical activation, raw material is thoroughly mixed with chemicals such as  $ZnCl_2$ ,  $H_3PO_4$ ,  $KOH$ ,  $NaOH$  etc. and pyrolysed in absence of air at higher temperature (Subramnian, 2007; Sharma, 2010; Hemashree, 2017). Chemical activation has advantages such as development of pore structure, lower energy cost and higher carbon yields; hence it is preferred to physical activation (Ma *et al.*, 2015; Prahas, 2008). Over the years microwave activation is gaining major interest in the production of carbon materials. Consumption of low energy and limited steps make microwave method very effective compared to the other methods (Menendez *et al.*, 2010).

Mustard seeds (Scientific name: *Brassica juncea*) are small, smooth, subglobose and brown in color. This seeds are used as spice in cooking and have also got medicinal importance. This seeds which are chief source of oil, contains glucosinolates, flavonoids, B-complex vitamins, and fatty acids like erucic, oleic, eicosenoic and palmitic acids (Levekar, 2007). From literature, many adsorption studies have been carried out using various forms of mustard, such as mustard oil cake (Rao *et al.*, 2010), de-oiled mustard cake (Katiyar *et al.*, 2015; Gupta *et al.*, 2010), mustard husk (Gautam *et al.*, 2013; Meena *et al.*, 2008), mustard waste ash (Singh *et al.*, 2013) and mustard stalk activated carbon (Ullhyan, 2014), which are extensively meant for the treatment of waste water and industrial effluents. As mustard seed is edible and has got medicinal properties, the prepared carbon might not have any nasty impact on health. Hence the activated carbon prepared from this seed could be used as potential adsorbent in food and pharmaceutical industries. So the study was carried out to prepare activated carbon from mustard seed and adsorption experiments were conducted to evaluate the adsorption capacity of prepared carbon. The present work is concerned with the preparation of activated

carbon from mustard seed by three different methods, its characterization and adsorption study.

## MATERIALS AND METHODS

### Preparation of activated carbon

The agricultural product, mustard seed is used in the current study for the synthesis of activated carbon. The mustard seeds were cleaned, washed with water to remove dirt and later dried in an oven at  $110^\circ C$  to remove moisture contents present in the sample. For physical activated carbon, carbonization of the mustard seed was carried out at  $400^\circ C$  for 1 hour in a muffle furnace and labelled as PMC. For chemical activation, the seed powder was pre-carbonized in a hot air oven and then treated with 10%  $ZnCl_2$  solution. The  $ZnCl_2$  treated sample was filtered, dried and carbonised at  $400^\circ C$  for one hour in muffle furnace. Obtained sample was washed with hot water and later with distilled water, oven dried and named as ZMC. Microwave activation was performed by using domestic microwave oven. The ground sample was irradiated for three hours at input microwave power 90 W (Energy  $\approx 270$  Joules/Sec) and the carbon obtained is labelled as MMC.

### Characterization of the activated carbon

The surface functional groups present on the activated carbon were identified by using IR Prestige-21 Fourier transform Infrared Spectrometer, Shimadzu (Japan). X-Ray diffraction study was performed by Rigaku Miniflex 600 (Japan). Thermo Gravimetric Analysis was performed by the instrument SDT Q600 V20.9 (Japan). The samples were heated in presence of nitrogen, at a rate of  $10^\circ C/min$  in a temperature range of  $25^\circ C$  to  $900^\circ C$ . SEM images were obtained using Sigma Series Field Emission Scanning Electron microscope (Zeiss).

### Adsorption studies

These activated carbons were used as an adsorbent for the adsorption of a dye, crystal violet and citric acid under various conditions such as contact time, temperature and concentration of the dye. For the adsorption study, a fixed amount of activated carbon (particle size  $100-50\mu m$ ) was added to an Erlenmeyer flask containing 50ml of the dye/acid solution. The dye/acid solution was stirred continuously for a definite period and filtered. The concentration of the filtered dye solution was determined spectrophotometrically. For the acid solution, concentration was determined by titrating the filtered solution with standardised sodium hydroxide solution. The amount of dye adsorbed,  $q_e$  (mg/g), by activated carbon at time  $t$ , was calculated by the eqn.

$$q_e = \frac{(C_o - C_e)V}{W} \quad (1)$$

where  $C_o$  and  $C_e$  are initial and equilibrium concentration (mg/L),  $V$  is volume of solution (L) and  $W$  is the mass of the adsorbate (g).

The amount of acid adsorbed,  $q_e$  by activated carbon was calculated by the equation:

$$q_e = \frac{(C_o - C_e)MV}{W} \quad (2)$$

where  $M$  is equivalent weight of acid.

## RESULTS AND DISCUSSION

### Characterization of Activated Carbon FTIR Spectroscopic Analysis

Figures 1–2 illustrates the FTIR spectra of raw mustard seed and activated carbons (PMC, ZMC, and MMC) prepared from mustard seed respectively. Absorption band formed in the region 3300–3400  $\text{cm}^{-1}$  (Fig. 1) may be due to merging of two peaks which corresponds to both O–H and N–H stretching. The band formed at 3008  $\text{cm}^{-1}$  is due to  $\text{sp}^2$  C–H stretching. The peaks at 2925  $\text{cm}^{-1}$  and 2856  $\text{cm}^{-1}$  correspond to asymmetric and symmetric stretching of  $-\text{CH}_2-$  respectively. The peak formed at 1747  $\text{cm}^{-1}$  is attributed to vibration of C=O bond. The bands at 1654  $\text{cm}^{-1}$  and 1542  $\text{cm}^{-1}$  may be due to bending of primary and secondary amine group respectively. The peaks formed at 1454  $\text{cm}^{-1}$  and 1376  $\text{cm}^{-1}$  are may be due to C–O–H vibration and  $\text{CH}_3$  bending respectively. C–N stretching is visible at 1240  $\text{cm}^{-1}$  and the peaks in the region 1200–1000  $\text{cm}^{-1}$  are due to C–O stretching (Viera *et al.*, 2009). The bands in the 1000–650  $\text{cm}^{-1}$  range can be due to out-of-plane bending of olefinic C–H groups and substituted aromatic rings (Kalsi, 2004; Lampman *et al.*, 2013).

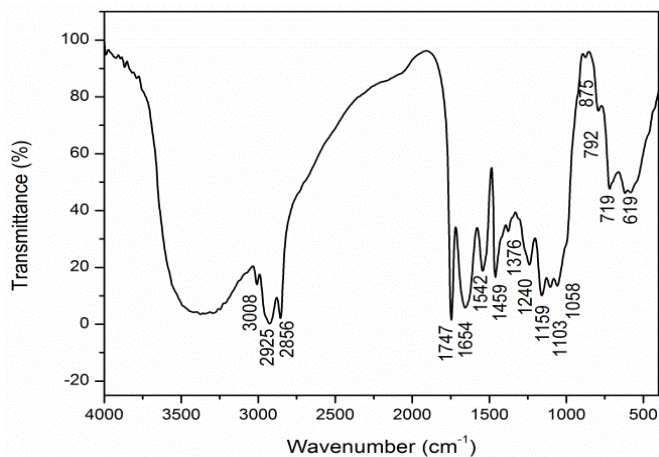


Fig. 1 FTIR spectrum for raw mustard seed.

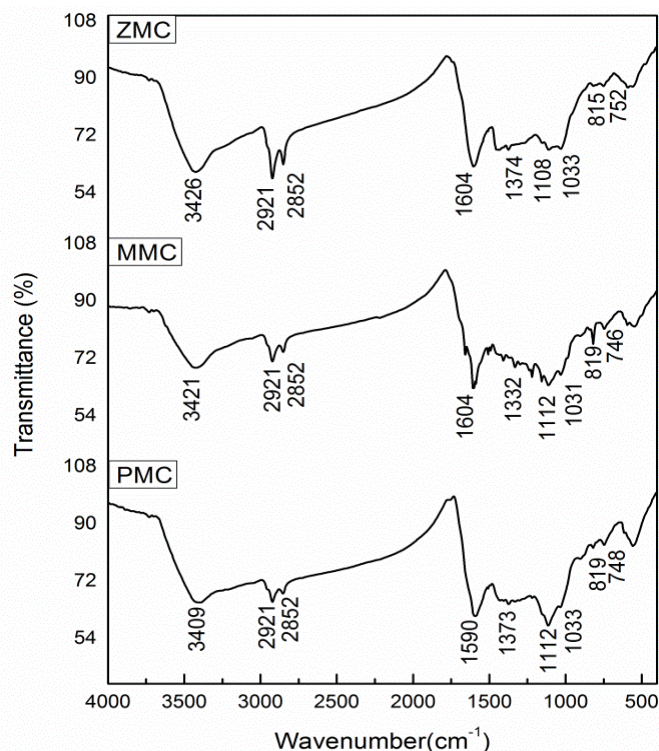


Fig. 2 FTIR spectra for activated carbon.

The obtained spectra of raw mustard seed and synthesised activated carbons were compared and a considerable difference was noticed between the IR spectra of these samples. The peaks which are characteristics of stretching mode of O–H, N–H, C–H and C–O–H bonds are continued to be present in the spectra of all the three activated carbons. At higher temperature, C=O group probably decomposes in to  $\text{CO}_2$ , CO and also C–O, C–N bonds of particular compounds are broken (Iyengar *et al.*, 1997), hence the peaks responsible for these particular groups are found missing in the IR spectra of all the three activated carbons. Hetero atoms like C, N, and O etc are unsaturated and plays active role in the adsorption process. The presence of several functional groups on the surface of activated carbon (NH,  $\text{CH}_3$ , OH etc) enhances the adsorptive capacity of an adsorbent hence the synthesised activated carbon can be considered as an effective adsorbent.

### X-Ray Diffraction Analysis

XRD method was used to study the characteristics of activated carbon. The X–ray diffractogram of the activated carbon is shown in Fig. 3.

It is clear from the figure that all the three activated carbon apparently showed amorphous nature. Peaks with noticeable intensities are considered to calculate inter planar distance  $d$ ,  $hkl$ , cell volume  $a^3$  and crystallite size  $D$  and the obtained results are shown in

**Table 1.** Bragg’s equation was used to determine inter planar distance *d*:

$$d = \frac{\lambda}{2\sin\theta} \tag{3}$$

where  $\lambda = 1.5418 \text{ \AA}$  (*CuK $\alpha$* ) and  $\theta$  is the scattering angle. The crystallite size was determined by the Scherrer equation:

$$D = \frac{K\lambda}{B \cos\theta} \tag{4}$$

where *B* is the half width of the peak and *K* = 0.9 is the shape factor (Prahas *et al.*, 2008).

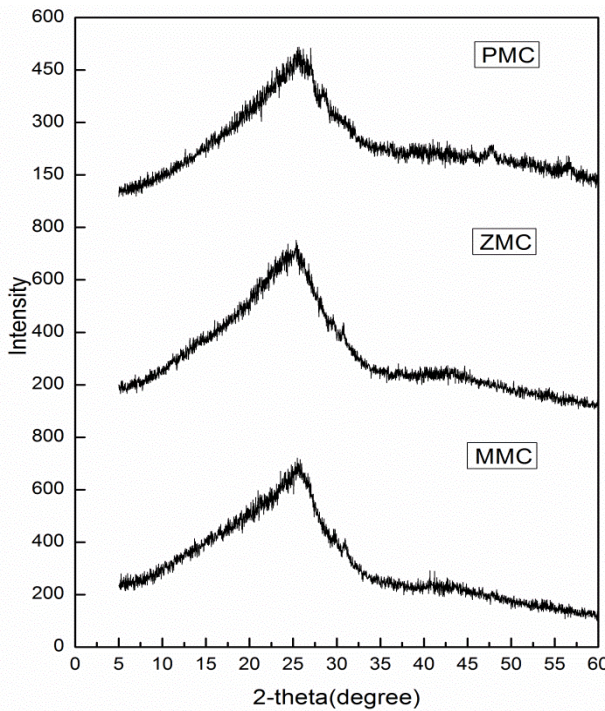


**Fig. 3** XRD of activated carbon (PMC, ZMC & MMC).

**Table 1.** XRD data for PMC, ZMC and MMC

Sample degree (A <sup>0</sup> )	2 $\theta$ (A <sup>0</sup> )	d	hkl	a (A <sup>0</sup> )	Cell Volume	Crystallite Size D
PMC	18.30	4.84	100	4.84	113.37	0.116
	24.40	3.64	110	5.07	130.32	0.117
	25.52	3.49	110	4.92	119.09	0.117
	26.16	3.40	110	4.79	109.90	0.118
ZMC	22.18	4.04	100	4.04	65.39	0.089
	23.84	3.73	100	3.73	51.89	0.089
	24.40	3.64	100	3.64	48.22	0.089
	25.36	3.51	100	3.51	43.24	0.089
	26.78	3.33	100	3.33	36.92	0.089
MMC	23.54	3.77	100	3.77	53.58	0.074
	24.40	3.64	100	3.64	48.22	0.074
	25.20	3.53	100	3.53	43.98	0.074
	25.80	3.45	100	3.45	41.06	0.075
	26.84	3.32	100	3.32	36.59	0.075

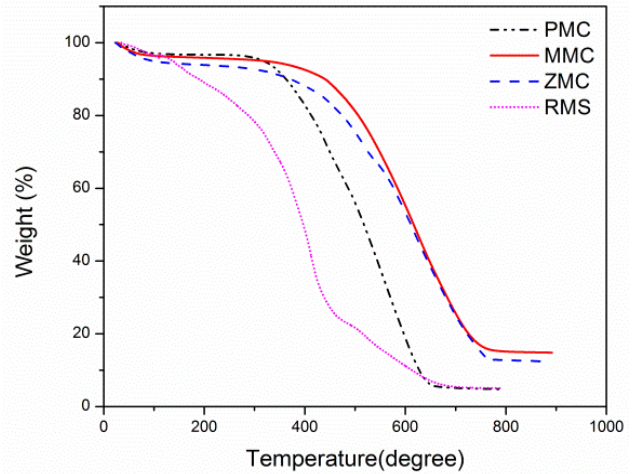


**Fig. 4** Thermo gravimetric curve of RMS and activated carbon.

Almost the same value for ‘*a*’ (**Table 1**) indicates the cubic pattern of the system. The values of crystallite size, *D* found to vary in the following order PMC>ZMC>MMC. It may be stated that MMC exhibits minimum *D* value with high surface area and is expected to be more active towards adsorption compared to other two activated carbons (PMC and ZMC).

**Thermo gravimetric analysis**

The TG curves obtained for raw mustard seed (RMS) and activated carbon (PMC, ZMC and MMC) are shown in **Fig. 4**. It is apparent that for raw mustard seed, weight loss occurs in three phases. The weight loss in the first phase may be due to dissipation of moisture present in the sample. In the second phase (110—300°C) the weight loss may be due to decomposition of some of the saturated and poly unsaturated fatty acids (palmitic acid, linoleic acid, myristic acid etc.) (Gouveia *et al.*, 2004) and the maximum weight loss in the third phase (300 - 650°C) may be the result of degradation of cellulose, and monounsaturated fatty acid (oleic acid, eurcic acid etc.) (Gouveia *et al.*, 2004; Yang *et al.*, 2007).

In case of the activated carbons, the weight loss in the range (20 - 130°C) is due evaporation of moisture. The gradual weight loss in the second phase (130 - 350°C) and sharp and maximum weight loss in the third phase (350 - 750°C) may be attributed to the decomposition of chemical components present in the activated carbon. Decomposition temperature of PMC, MMC and ZMC specifies that zinc activated and microwave activated carbons exhibit higher stability than the physical activated carbon.

**Scanning Electron Microscopic Analysis**

SEM micrographs displayed the surface morphologies of activated carbon before and after adsorption. **Figure 5a** showed that the microwave treated carbon has heterogeneous surface with several irregular pores of different size. **Figure 5b–5c** are the post adsorption images, and it is clear from the image that after the adsorption, the pores are clogged up with dye/acid molecules. During adsorption, adsorbate moves into the carbon pores and results in the pore blockage.

**ADSORPTION STUDIES**

**Adsorption Isotherms**

The adsorption isotherm was studied by Langmuir, Freundlich and BET isotherm models. The Langmuir isotherm is based on the assumption that adsorption cannot proceed beyond monolayer coverage and all the active sites are equivalent on uniform surface (Atkins *et al.*, 2002). The linear form of Langmuir equation can be expressed as (Hameed *et al.*, 2008):

$$\frac{C_e}{q_e} = \frac{1}{K_L q_{max}} + \frac{1}{q_{max}} C_e \tag{5}$$

where  $C_e$  is the equilibrium Concentration (mg/L),  $q_e$  is the amount of adsorbate adsorbed (mg/g),  $q_{max}$  is the monolayer capacity (mg/g) and  $K_L$  is the adsorption equilibrium constant (L/mg). The values of  $q_{max}$  and  $K_L$  were calculated by the slope and intercept obtained from the plot of  $C_e/q_e$  vs.  $C_e$ . The nonlinear plot (**Fig. 6**) indicated that Langmuir isotherm does not fit well for the obtained data.

The Freundlich isotherm has been used principally for adsorption from solution (Barrow 1992). The linear form of the Freundlich Isotherm is represented as: (Netpradit *et al.*, 2004):

$$\log q_e = \log K_f + \frac{1}{n} \log C_e \tag{6}$$

where  $n$  shows the adsorption intensity in the Freundlich equation and  $K_f$  is the Freundlich adsorption capacity [(mol/g)(L/g)<sup>1/n</sup>]. The values of  $n$  and  $K_f$  were calculated by the slope and intercept obtained from the plot of  $\log q_e$  vs.  $\log C_e$  (**Fig. 7**).

BET provides information related to multilayer adsorption behaviour and monolayer adsorption capacity (Ebadi *et al.*, 2009). The linear form of the BET isotherm model (Foo *et al.*, 2012) for liquid-solid interface may be written as:

$$\frac{C_e}{q_e(C_s - C_e)} = \frac{1}{q_s C_{BET}} + \frac{C_{BET} - 1}{q_s C_{BET}} \left( \frac{C_e}{C_s} \right) \tag{7}$$

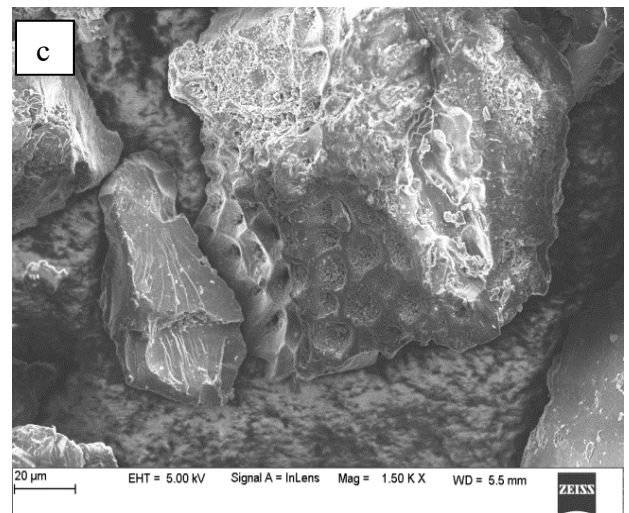
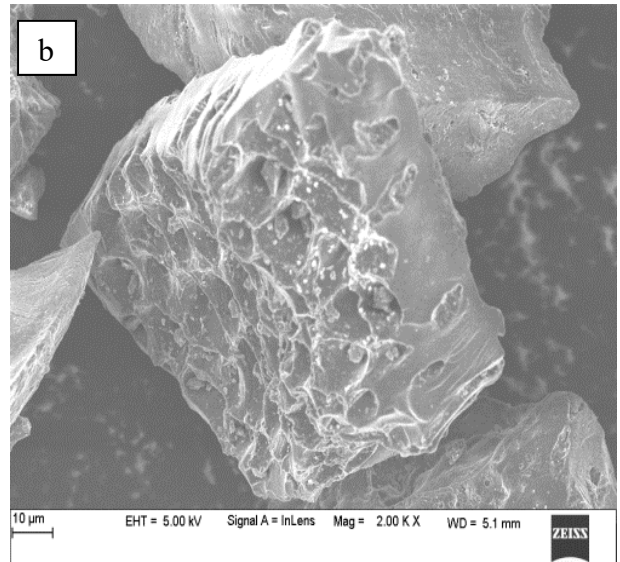
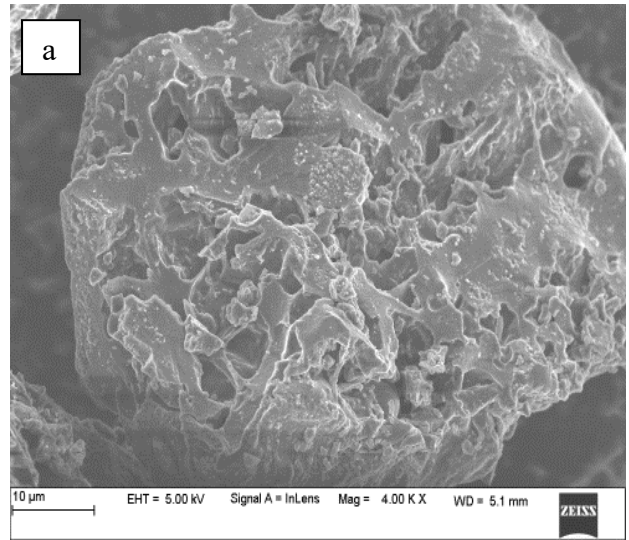


**Fig. 5** Scanning Electron Micrographs of Microwave activated carbon. (a) before adsorption (b) after adsorption of CV (c) after adsorption of CA.

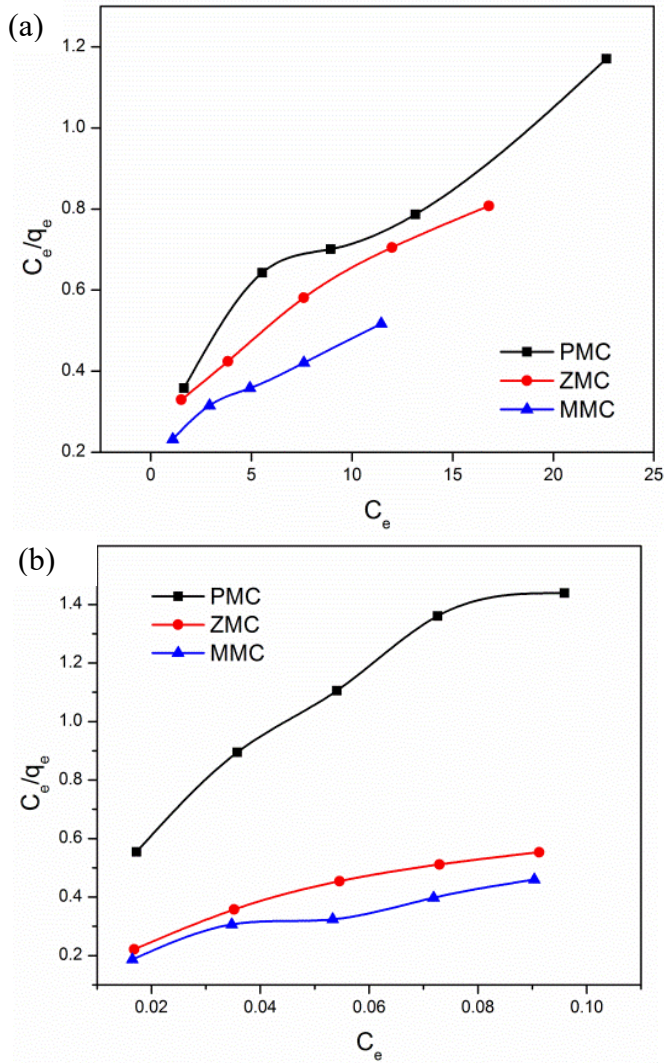


Fig. 6 (a) Langmuir Isotherm for CV adsorption and (b) CA adsorption.

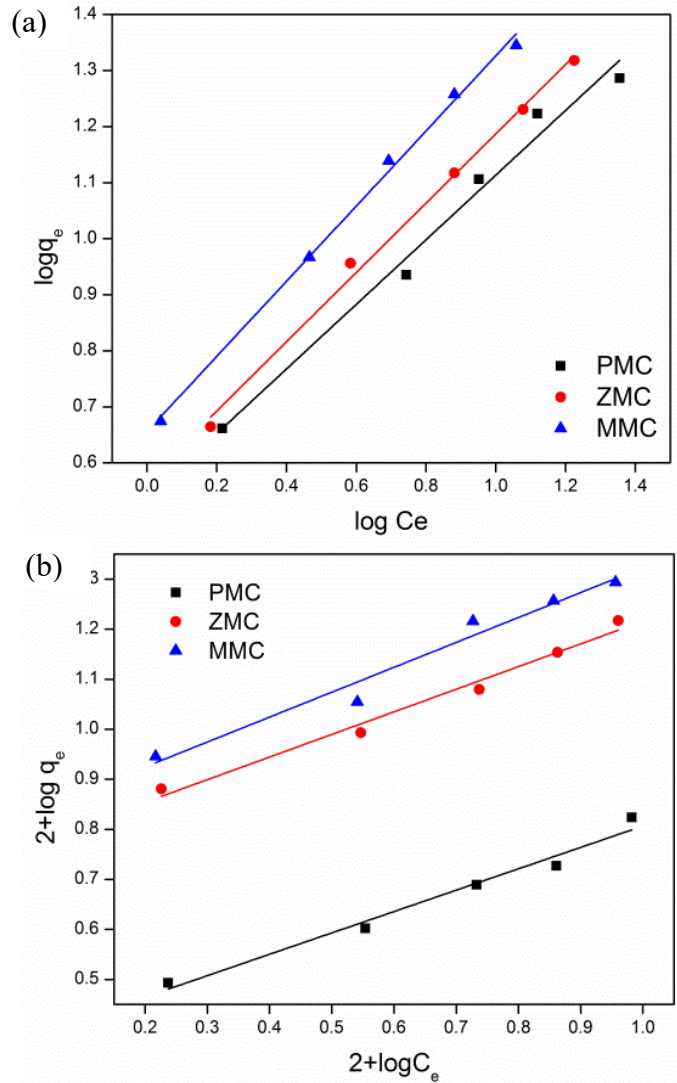


Fig. 7 (a) Freundlich Isotherm for CV adsorption and (b) CA adsorption.

where  $q_e$ ,  $q_s$ , are the equilibrium adsorption capacity (mg/g), theoretical isotherm saturation capacity(mg/g) respectively,  $C_s$  is the adsorption monolayer saturation concentration(mg/L), and  $C_{BET}$  is BET adsorption isotherm (L/mg).  $C_{BET}$  can be determined from the intercept of the linear plot of  $\left(\frac{C_e}{C_s - C_e}\right)\left(\frac{1}{q_e}\right)$  vs.  $\frac{C_e}{C_s}$  and also  $q_s$  values were calculated using the equation:

$$q_s = \frac{1}{slope + intercept} \quad (8)$$

The data obtained for both acid and dye system was best interpreted by the Freundlich isotherm model. The value of  $n$  is found to be greater than unity (Table 2) which strongly suggests that the adsorption process is favourable. Freundlich isotherm fits well with the obtained adsorption data, so it can be said that multilayer

Table 2 Freundlich and BET constants for the adsorption of crystal violet and citric acid

Sample	Freundlich Constant			BET Constant	
	$K_f$	$n$	$R^2$	$C_{BET}$	$q_s$
1. CV					
PMC	1.71	1.73	0.98	0.010	8.60
ZMC	1.76	1.61	0.99	0.009	8.81
MMC	1.93	1.49	0.99	0.012	9.08
2. CA					
PMC	2.39	2.34	0.97	-2.65	0.02
ZMC	5.79	2.21	0.98	-1.74	0.04
MMC	6.68	2.00	0.96	-0.28	0.06

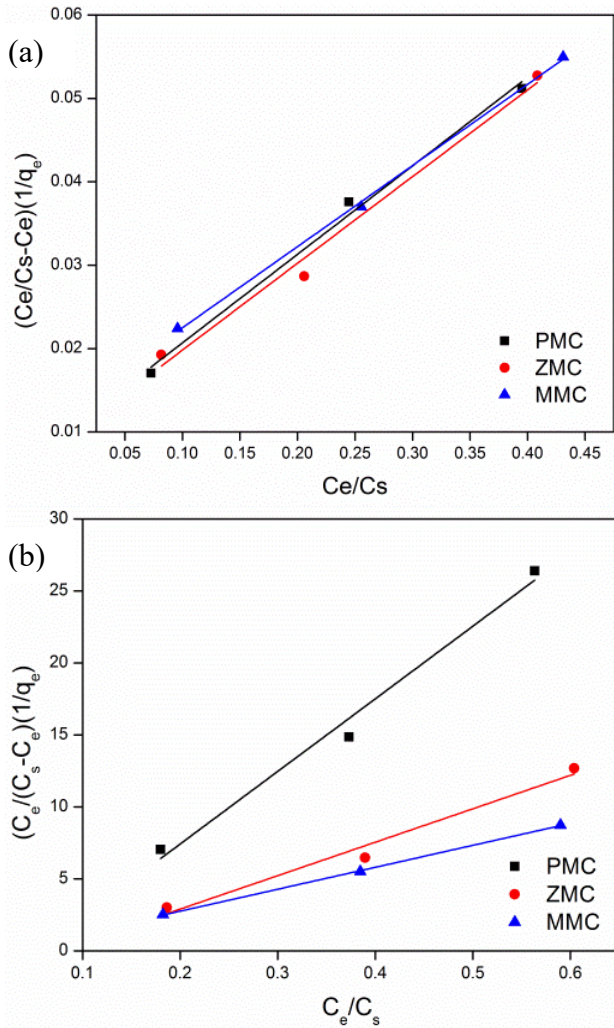


Fig. 8 (a) BET Isotherm for Crystal violet and (b) Citric acid adsorption.

adsorption might have taken place at heterogeneous sites on the surface of the adsorbent (Gautam *et al.*, 2013). The validity of BET equation was tried for the both the system, in the range of 20- 60 ppm. Linear plot (Fig. 8) showed the applicability of the BET isotherm for the dye system where as negative intercept indicated that it is not valid for citric acid adsorption.

**Effect of contact time**

The influence of time for intake of dye and acid was studied by carrying out adsorption experiments at different time intervals with fixed quantity of adsorbent. It is apparent from Fig. 9 that the adsorption of crystal violet is rapid during initial stage and gradually slows down with the time, whereas for acid, adsorption slowly increased and remained almost constant for all the three carbons. The increase in the adsorption rate at the initial stage is due the presence of large number of active centres on the surface of activated carbon. A similar phenomenon was observed in the adsorption of Alizarin Red S on mustard husk by R. K. Gautam *et al.* (2013).

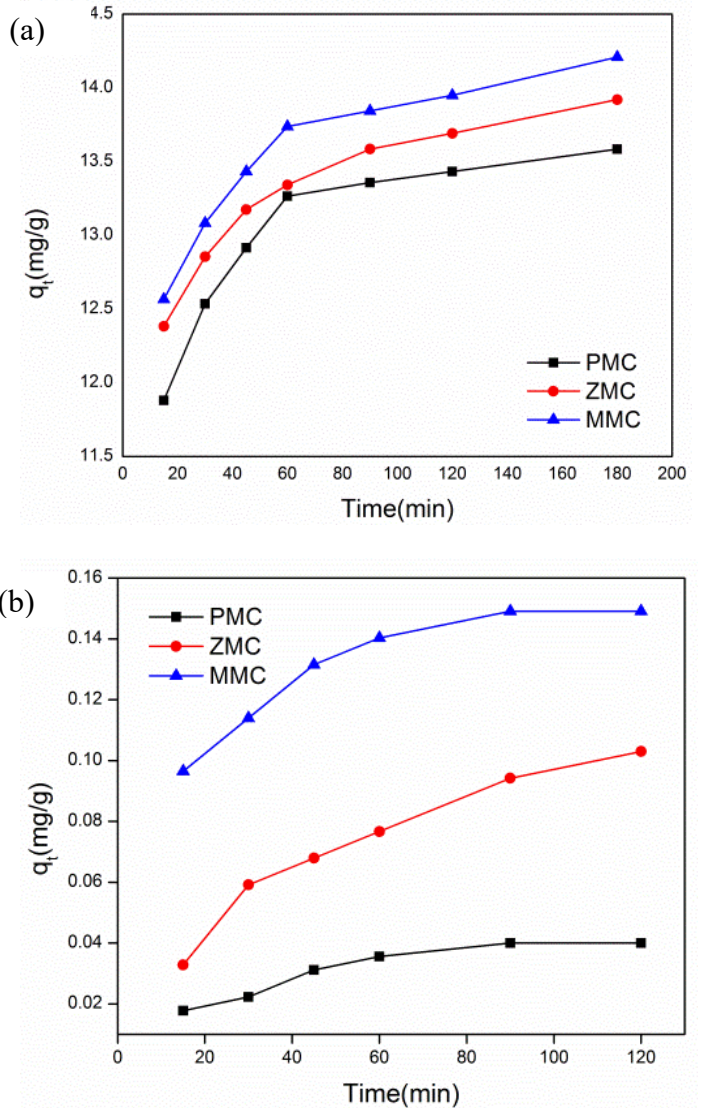


Fig. 9 (a) Plot of contact time Vs adsorption of CV and (b) Plot of contact time Vs adsorption of CA.

**Adsorption Kinetics**

The kinetic models, first order and second order were utilized to study the adsorption process. Lagergren proposed first order kinetic model as given below: (Banerjee *et al.*, 2016)

$$\log(q_e - q_t) = \log q_e - \frac{k_1}{2.303} t \tag{9}$$

where  $k_1$  ( $\text{min}^{-1}$ ) is the rate constant of the first order adsorption and  $q_t$  is the adsorption capacity at time (mg/g). The rate parameters  $k_1$  and  $q_e$  can be obtained from the intercept and slope of the plot of  $\log(q_e - q_t)$  vs time. The lower correlation value,  $R$  suggested that the first order model is inappropriate to describe kinetics of the system. The second - order kinetic model (Wu *et al.*, 2001) is expressed by:

$$\frac{t}{q_t} = \frac{1}{k_2 * q_e^2} + \frac{t}{q_e} \quad (10)$$

where  $q_e$  and  $q_t$  are the adsorption capacities at equilibrium and time,  $t$  respectively(g/mg) and  $k_2$  is the equilibrium rate constant of second order adsorption. The rate constant  $k_2$  was obtained from the slope and intercept from the plot of  $t/q_t$  vs.  $t$  (Fig. 10).

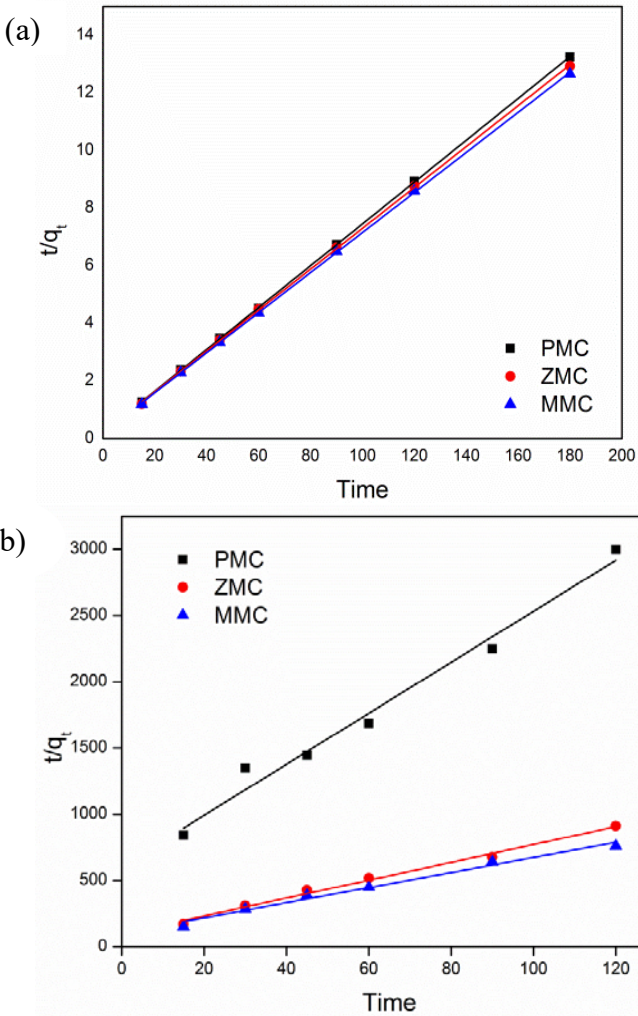


Fig. 10 (a) Plot of Second-order kinetic modelling for CV adsorption and (b) CA adsorption.

Correlation coefficient values (Table 3) are found to be 0.99 for dye and 0.98-0.99 for acid system, for all the three carbon which indicates that the system follows second order kinetic model. It was also found that adsorption capacity,  $q_e$  is high for crystal violet and this could be due to effectual interaction between the functional groups present on the carbon surface and dye molecules.

Table 3 Second order rate constants for the adsorption

Sample	Crystal Violet			Citric Acid		
	$k_2$	$q_e$	$R^2$	$k_2$	$q_e$	$R^2$
PMC	0.267	13.77	0.99	0.611	0.052	0.98
ZMC	0.023	14.09	0.99	0.464	0.148	0.99
MMC	0.028	14.49	0.99	0.312	0.175	0.98

Effect of Temperature

Influence of temperature on the adsorption was carried out in the temperature range 10 - 60°C. The results indicated that, for both the system adsorption increased with the rise in temperature with a later decrease (Fig. 11). The initial rise in adsorption capacity may be due to increase in the mobility of the dye/acid molecules as well as increase in the pore size of the adsorbent with an increase in temperature (Saeed *et al.*, 2010). The increase in temperature makes the adsorption process easier by decreasing the  $E_a$  till 40°C. The later decrease in the adsorption capacity may be a consequence of initiation of desorption. The decrease in adsorption capacity with as the two factors which influence increase in temperature is due to weakening of the

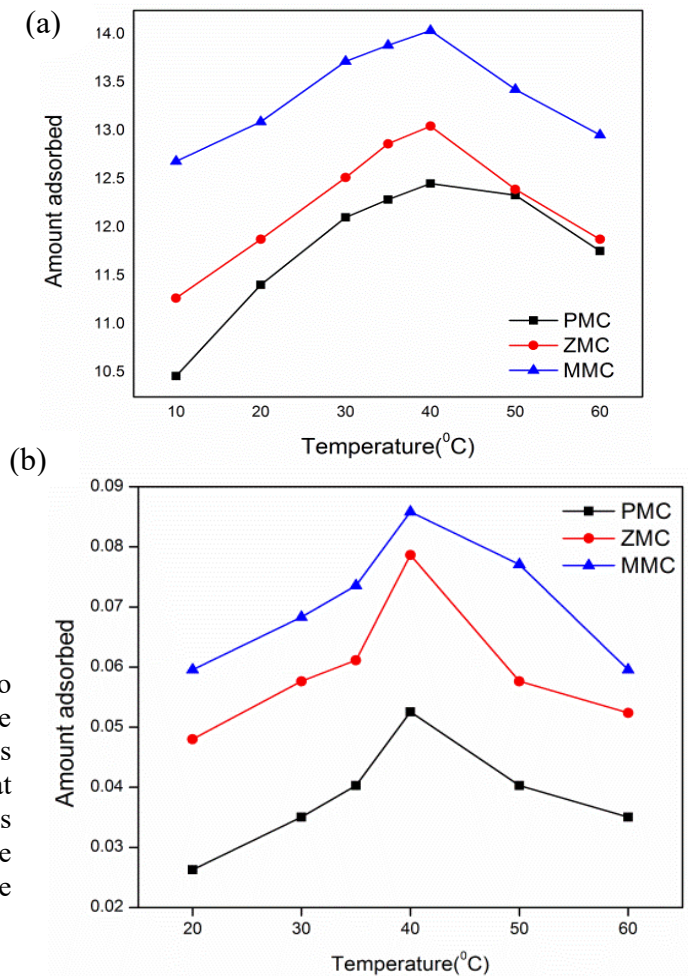


Fig. 11 (a) Effect of temperature for CV adsorption and (b) for CA adsorption.

interaction between the adsorbent and dye/acid molecules, and also between adjacent molecules on the adsorbed phase (Ofomaja *et al.*, 2007). So it may be stated that desorption comes in to picture after 40<sup>0</sup>C.

**Adsorption Thermodynamic**

Experiments were carried out at different temperature to determine the thermodynamic parameters  $\Delta H^\circ$ ,  $\Delta S^\circ$  and  $\Delta G^\circ$  for the adsorption. The standard enthalpy and entropy of the adsorption process can be calculated from the following equation:

$$\Delta G^\circ = RT \ln K_c \tag{11}$$

$$\ln K_c = \frac{-\Delta H^\circ}{RT} + \frac{\Delta S^\circ}{R} \tag{12}$$

where  $R$  is the gas constant,  $T$  is the absolute temperature and  $K_c$  is the equilibrium constant which is obtained from the following equation:

$$K_c = \frac{q_e}{C_e} \tag{13}$$

where  $q_e$  is the amount adsorbed on adsorbent at equilibrium and  $C_e$  is the equilibrium concentration of dye/acid in the solution. The values of  $\Delta H^\circ$  and  $\Delta S^\circ$  were calculated from the linear plot of  $\ln K_c$  vs.  $1/T$  (Fig. 12) and the results obtained are given in Table 4.

Positive values of  $\Delta H^\circ$  (Table 4) indicate that the adsorption process is endothermic and the low values  $\Delta H^\circ$  specify that the system experience physisorption with the formation of multilayer of adsorbate on adsorbent, which supports the previous conclusion, made under adsorption isotherm study. Small positive values of  $\Delta S^\circ$  indicate the instability of adsorbed species on the surface compared to the bulk. The negative value of  $\Delta G^\circ$  implies that the adsorption process is spontaneous.

**Mechanism of Adsorption**

Generally carboxyl, carbonyl and phenolic hydroxyl are the most common surface groups which are responsible for the adsorption (Mittal, 2007). In the present case, FTIR studies showed that the prepared carbon exhibited the presence of functional groups such as OH, NH and COH. Hydrogen bonding and electrostatic interaction between these surface groups of the carbons and the dye/acid molecule can be considered.

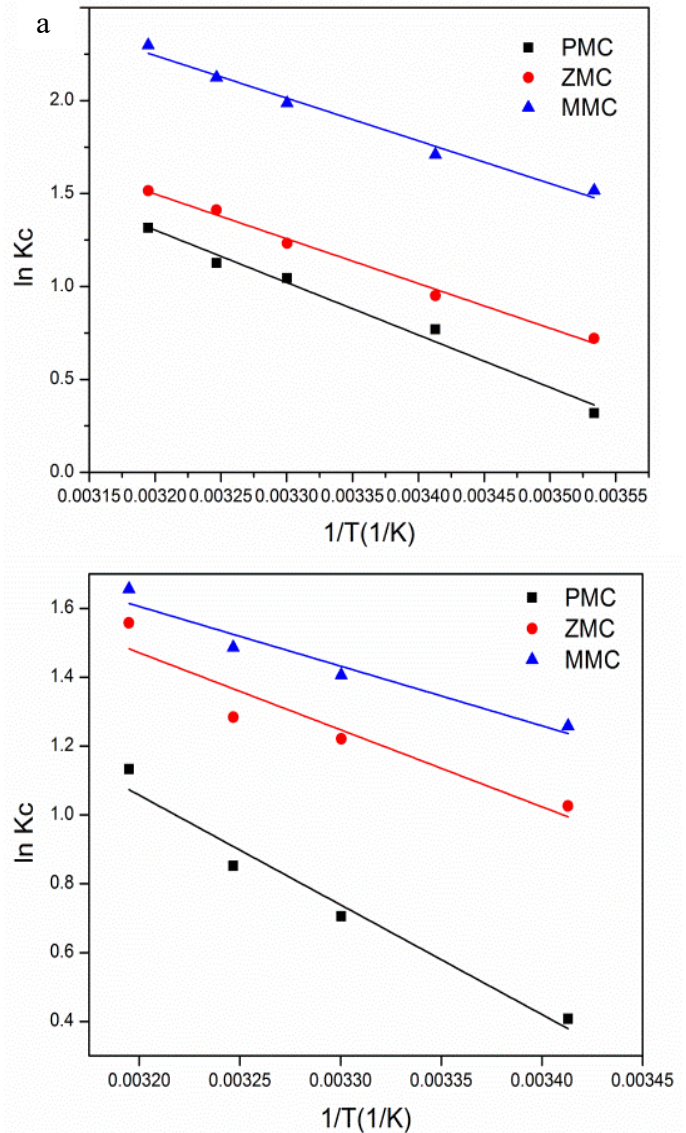
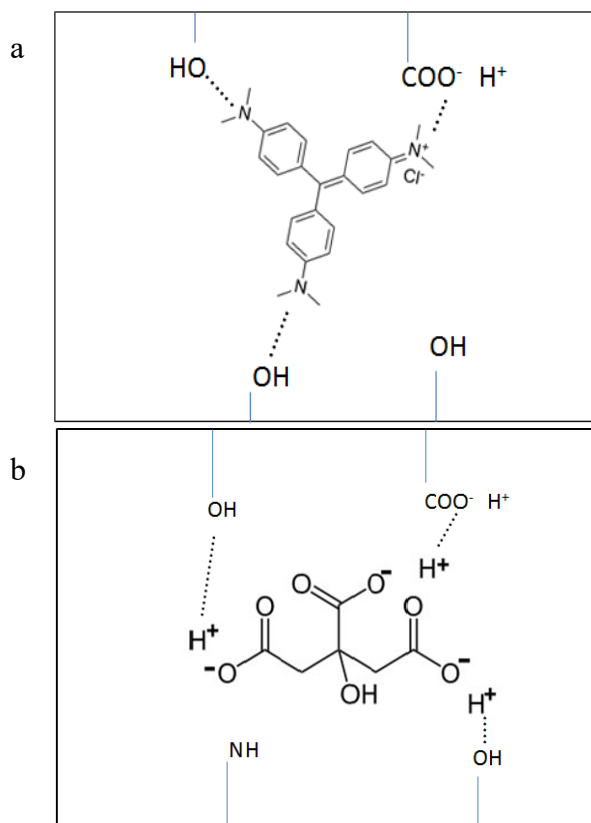


Fig. 12 (a) van't Hoff equation for CV adsorption and (b) Citric acid adsorption.

Table 4 Thermodynamic parameters for the Adsorption of CV and CA on activated carbon

Sample	$\Delta H^\circ$ (kJ/mol)	$\Delta S^\circ$ (kJ/mol/K)	$E_a$	$\Delta G^\circ$ (kJ/mol)	$K_{ads}$ (kJ/mol)
<b>1. CV</b>					
PMC	23.46	0.085	25.95	- 2.27	1.002
ZMC	20.01	0.076	22.50	- 2.93	1.003
MMC	19.09	0.079	21.58	- 4.60	1.004
<b>2. CA</b>					
PMC	26.48	0.093	29.00	- 1.81	1.001
ZMC	18.60	0.071	21.13	- 3.18	1.002
MMC	14.40	0.060	16.93	- 3.66	1.003



**Fig. 13** (a) Probable mechanism for the adsorption of CV (b) CA on to activated carbon.

the adsorption process (Bharati *et al.*, 2013). The probable interaction between the surface functional groups of the carbon and the dye/acid molecule is shown in **Fig. 13**. A considerable difference was observed between the adsorption capacity of the crystal violet and citric acid. Adsorption capacity of citric acid was found to be less compared to the dye used. The reduction in the adsorptive behavior of citric acid may be due to its weak dissociation.

## CONCLUSION

Activated carbon were synthesised from mustard seed by three different methods, characterized and utilized for adsorption study. The adsorption process was influenced by concentration, time as well as temperature. Data acquired from the concentration variation fits well with Freundlich Isotherm. The system followed second order rate. The positive value of  $\Delta H^0$  indicated that the adsorption is endothermic. The adsorption capacity of crystal violet found to be much higher than citric acid and also it is concluded that MMC is most efficient adsorbent for the dye adsorption.

**ACKNOWLEDGMENT** The authors are thankful to the Coordinator, DST- FIST Program, USIC and DST – PURSE, Mangalore University for providing

instrumental facilities to the carry out the present research work. The authors are also thankful to UGC – SAP, Delhi for financial assistance to carry out the present research work.

## REFERENCES

- Atkins, P., Paula, J. (2002) Atkins' Physical Chemistry, Seventh Edition, Oxford University Press.
- Barrow, G. M. (1992) Physical Chemistry, Fifth Edition, McGraw – Hill Edition.
- Banerjee, S., Gautam, R. K., Rai, P., Chattopadhyaya, M. C. (2016) Adsorptive removal of toxic dyes from aqueous phase using notorious weed *Lantana camara*(Linn.) as biosorbent, *Res Chem Intermed.* 42: 5677-5708. doi.10.1007/s11164-015-2397-3
- Bharathi, K.S., Ramesh, S.T. (2013) Removal of dyes using agricultural waste as low-cost adsorbents: a review *Appl Water Sci.* 3:773-790. doi.10.1007/s13201-013-0117-y
- Ebadi, A., Jafar, S., Mohammadzadeh, Khudiev, A. (2009) What is the correct form of BET isotherm modelling liquid phase adsorption? *Adsorption* 15: 65-73. doi.org/10.1007/s10450-009-9151-3
- Foo, K.Y., Hameed, B. H. (2010) Insight in to the modelling of adsorption isotherm systems *Chem. Eng. J.* 156:2-10. doi:10.1016/j.ccej.2009.09.013
- Gautam, R. K., Mudhoo, A., Chattopadhaya, M C. (2013) Kinetic, equilibrium, thermodynamic studies and spectroscopic analysis of Alizarin Red S by removal by mustard husk, *JECE*, 1, 1283-1291. doi.org/10.1016/j.jece.2013.09.021
- Glasstone, S. (1981) Text book of Physical Chemistry, Second Edition, The MacMillan Company of India.
- Gupta, V. K., Jain, R., Malathi, S., Nayak, A. (2010) Adsorption – desorption studies of indigo carmine from industrial effluents by using deoiled mustard and its comparison with charcoal, *J. Colloid Interface Sci.*, 348: 628-633. doi:10.1016/j.jcis.2010.04.085
- Gouveia de Souza et al. (2004) A Thermoanalytic and Kinetic study of Sunflower oil, *Brazilian Journal of Chemical Engineering*, 21: 265–273. doi.org/10.1590/S0104-66322004000200017
- Hameed, B.H., Daud, F.B.M. (2008) Adsorption studies of basic dye on an activated carbon derived from agricultural waste: *Hevea brasiliensis* seed coat *Chem. Eng. J.* 139:48 – 55. doi.org/10.1016/j.ccej.2007.07.089
- Hemashree K., J. Ishwara Bhat (2017) Synthesis, characterization and adsorption behaviour of coconut leaf carbon. *Res Chem Intermed* 43:4369–4386. DOI 10.1007/s11164-017-2883-x
- Iyengar, G. V. et al. (1997) Element Analysis of Biological Samples principles and practice, Vol 2, CRC Press.
- Kalsi, P.S. (2004) Spectroscopy of Organic Compounds, Sixth Edition, New Age International Publisher
- Katiyar, A, Singh, A. K., Joshi, A. (2015) Utilization of waste material (Part II): DMAC (De-oiled mustard cake), as an efficient adsorbent for the removal of metal cutting fluids from aqueous medium/industrial waste water, *IJETR*,3:131-137, ISSN:2321-0869
- Lampman, G.M., Pavia, D.L., Kriz, G.S., Vyvyan, J. R. (2013) Spectroscopy, Fourth Edition, Cengage Learning
- Levekar, G.S. (2007) Database on Medicinal Plants Used in Ayurveda & Siddha, Volume – 8, Central Council for Research in Ayurveda Siddha, New Delhi
- Ma, Y., Wang, Q., Wang, X., Sun, X., Wang, X. (2015) A comprehensive study on activated carbon prepared from spent shiitake substrate via pyrolysis with ZnCl<sub>2</sub>. *J Porous Mater.* 22:157-169. DOI 10.1007/s10934-014-9882-8

- Meena, A. K., Kadirvelu, K., Mishra, G. K., Rajagopal, C., Nagar, P. N. (2008) Adsorption of Pb(II) and Cd(II) metal ions from aqueous solutions by mustard husk, *J. Hazard. Mater* 150: 619–625. DOI: 10.1016/j.jhazmat.2007.05.011
- Menendez, J.A., Arenillas, A., Fidalgo, B., Fernandez, Y., Zubizarreta, I., Calvo, E. G., Bermudez, J.M. (2010) Microwave heating process involving carbon materials, *Fuel Process. Technol.* 91:1-8. doi.org/10.1016/j.fuproc.2009.08.021
- Mittal, A., Kurup, L., Mittal, J. (2007) Freundlich and Langmuir adsorption isotherm and kinetics for the removal of tartazine from aqueous solutions using hen feathers. *J. Hazardous Materials*, 146:243-248. DOI: 10.1016/j.jhazmat.2006.12.012
- Netpradit, S., Thiravetyan, P., Towprayoon, S. (2004) Adsorption of three azo reactive dyes by metal hydroxide sludge: effect of temperature, pH and electrolytes, *J Colloid Interface Sci.* 270: 255 – 261, doi:10.1016/j.jcis.2003.08.073
- Ofomaja, A. E., Ho, Y. (2007) Equilibrium sorption of anionic dye from aqueous solution by palm kernel fibre as sorbent, *Dyes and Pigments*, 74: 60–66. doi:10.1016/j.dyepig.2006.01.014
- Prahas, D., Kartika, Y., Indraswati, N., Ismadji S., Activated carbon from jackfruit peel waste by H<sub>3</sub>PO<sub>4</sub> chemical activation: Pore structure and surface chemistry characterization *Chem. Eng. J.* 140:32-42 (2008). doi:10.1016/j.cej.2007.08.032
- Raj, G. (1991) Surface Chemistry (Adsorption), Goel Publishing House Meerut
- Rao, R. A. K., Khan, M. A., Byong – Hun – Jeon (2010) Utilization of carbon derived from mustard oil cake (CMOC) for the removal of bivalent ions: Effect of anionic surfactant on the removal and recovery. *J. Hazard. Mater* 173: 273-282. DOI: 10.1016/j.jhazmat.2009.08.080
- Saeed, A., Sharif, M., Iqbal, M (2010) Application potential of grapefruit peel as dye adsorbent: Kinetics, equilibrium and mechanism of crystal violet adsorption *J. Hazard. Mater.* 179:564–572. doi: 10.1016/j.jhazmat.2010.03.041
- Sawyer, C. N., McCarty, P. L., Parkin, G.F. (1994) Chemistry for Environmental Engineering, Fourth Edition, McGraw- Hill international Editions, Singapore
- Sharma, Y.C., Uma and Gode, F. (2010) Engineering Data for optimization of preparation of activated carbon from an economically viable material, *J. Chem. Eng. Data*, 55, 3991-3994. doi.10.1021/je100041x
- Singh, H, Samiksha, Roohi, S. (2013) Removal of basic dyes from aqueous solutions using mustard waste ash and buffalo dung ash, *IJES* 3,1711-1725. doi:10.6088/ijes.2013030500039
- Song, X., Zhang, Y. and Chang C. (2012) Novel method for preparing activated carbons with high specific surface area from rice husk *Ind. Eng. Chem. Res.* 51:15075-15081. dx.doi.org/10.1021/ie3012853
- Subramanian, V. et al. (2007) Super capacitors from activated carbon derived from banana fibres, *J. Phys. Chem. C* 111, 7527-753. DOI: 10.1021/jp067009t
- Sudha, R., Srinivasan, K., Premkumar, P. (2016) Kinetic, mechanism and equilibrium studies on removal of Pb(II) using Citrus limettioides peel and seed carbon, *Res Chem Intermed*, 42:1677-1697. DOI 10.1007/s11164-015-2111-5
- Ullhyan, A. (2014) Adsorption of reactive blue-4 dye from aqueous solution on to acid activated mustard stalk: Equilibrium and Kinetic studies, *GJBAHS*, 3: 98-105, ISSN: 2319-5584
- Vieira, A. P. et al. (2009) Kinetics and thermodynamics of textile dye adsorption from aqueous solutions using babassu coconut mesocarp (2009) *J. Hazard. Mater.* 166:1272 – 1278. doi: 10.1016/j.jhazmat.2008.12.043
- Wu, F., Tseng, R. and Juang, R. (2001) Kinetic Modelling of Liquid –Phase adsorption of Reactive Dyes and metal ions on Chitosan, *Wat. Res.* 3:613-618, PII: S0043-1354(00)00307-9
- Yang, H., Yan, R., Chen, H., Lee, D. H., Zheng, C. (2007) Characteristics of hemicellulose, cellulose and lignin pyrolysis, *Fuel*, 86:1781-1788. doi:10.1016/j.fuel.2006.12.013